Contrib Mineral Petrol (1994) 115:356–366

Contributions to Mineralogy and Petrology

Nd, Pb and Sr isotopic data from the Napak carbonatite-nephelinite centre, eastern Uganda: an example of open-system crystal fractionation

Antonio Simonetti and Keith Bell

Ottawa-Carleton Geoscience Centre, Department of Earth Sciences, Carleton University, Ottawa, Ontario K1S 5B6, Canada

Received June 30, 1992 / Accepted May 25, 1993

Abstract. Nd, Pb and Sr isotopic data from nephelinite lavas from the Tertiary nephelinite-carbonatite complex of Napak, eastern Uganda, show large isotopic variations that can only be attributed to open-system behaviour. Possible explanations of the data include mixing between nephelinitic melts derived from an isotopically heterogeneous mantle, or interaction between a HIMU melt and mafic granulites. In both models crystal fractionation, involving olivine and clinopyroxene, played an important role. Major element chemistry, textural evidence and isotopic data from clinopyroxene phenocrysts from the olivine-bearing nephelinites, suggest that the pyroxenes did not crystallize from their host liquids. The isotopic data from the clinopyroxene phenocrysts support an interpretation of crystal fractionation in an open magma system that was undergoing continuous isotopic change. This study emphasises the importance of using combined isotopic data from both whole rock and mineral phases to interpret the evolutionary history of a single eruptive centre.

Introduction

Within the past decade, numerous isotopic and trace element studies have attempted to decipher the sources of various basaltic magmas but most of these have concentrated on oceanic areas, particularly the mantle sources that produced mid-ocean ridge (MORB), and oceanic island basalts (OIB). More controversial are the origin and evolution of continental volcanics, particularly, alkali basalts and nephelinites, and the nature of their mantle sources. The chemical and petrological features from such studies are commonly cited as evidence for a large-ion-lithophile element (LIL)-enriched mantle (eg. Lloyd and Bailey 1975; Frey et al. 1978). Nephelinites, with high Mg numbers [100.Mol MgO/(Mol MgO + Mol FeO), > 68], probably represent primary mantle melts. Experiments carried out up to 36 kbar have shown that nephelinitic magmas cannot be in equilibrium with a lherzolitic mantle source (Bultitude and Green 1968, 1971; Allen et al. 1975; Merrill and Wyllie 1975), but are probably the products of small (< 5%) degrees of partial melting of a carbonated (high CO_2/H_2O ratio) peridotite or pyrolite at high pressures (Brey and Green 1977; Brey 1978; Olafsson and Eggler 1983; Wallace and Green 1988). Experimental results are consistent with derivation of a primary nephelinitic liquid from an amphibole peridotite at pressures of 20 to 25 kbar (Olafsson and Eggler 1983; Eggler 1989).

The eastern branch of the East African Rift Valley System is associated with numerous recent nephelinite-carbonatite volcanic centres (Fig. 1), and provides a unique setting for studying the chemical evolution of the sub-continental upper mantle. The volcanic centres of eastern Uganda are particularly well suited for isotopic investigation because of their wide compositional range (melilite nephelinite, olivine nephelinite, melanephelinite, phonolite), and their relatively young ages. The K-Ar dates from carbonatite centres in eastern Uganda and nearby parts of Kenya range from 32 to 7 Ma (Bishop et al. 1969; Baker et al. 1971; Cahen et al. 1984).

Napak is unique among the many eastern Ugandan nephelinite-carbonatite centres, because both extrusive and intrusive rocks are preserved (Fig. 2). A Lower Miocene age for some of the early Napak volcanic activity was based on mammalian fossil remains found in tuffs and agglomerates (Bishop 1958), and this was supported by K-Ar whole rock, biotite and nepheline dates (Bishop et al. 1969) from tuffs, lavas and the central ijolite plug that range from 30 to 7 Ma. The spread in dates may be the result of either excess argon, or of argon loss (Bishop et al. 1969).

The carbonatite-ijolite central plug at Napak is flanked by interlayered, deeply dissected agglomerates, tuffs and silica-undersaturated lava flows (Fig. 2, King 1949) that overlie quartzo-feldspathic gneissic and granulitic Precambrian basement. Pyroclastic rock make up 97% of Napak and the remainder consist of silica-undersaturated lavas, mostly nephelinitic in composition (King 1949).

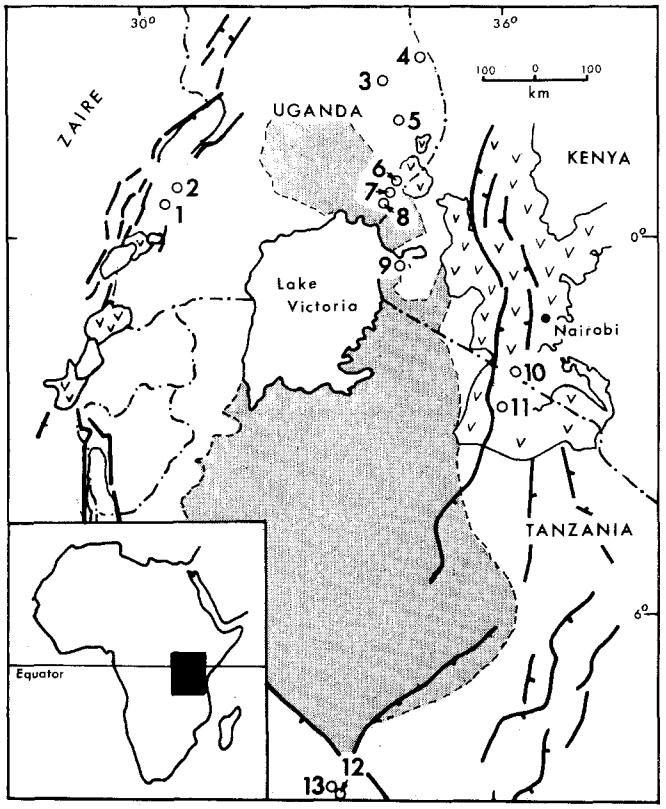

Fig. 1. Regional geology of East Africa showing the Tanzanian Shield, *shaded area*, and the East African Rift Valley System (after Bell and Blenkinsop 1987). Also shown is the distribution of some of the Tertiary and Recent carbonatite-nephelinite centres: *1*, Kalyango; *2*, Rusekere; *3*, Toror; *4*, Moroto; *5*, Napak; *6*, Bukusu; *7*, Tororo; *8*, Sukulu; *9*, Homa Bay; *10*, Shombole; *11*, Oldoinyo Lengai; *12*, Panda Hill; *13*, Sengeri

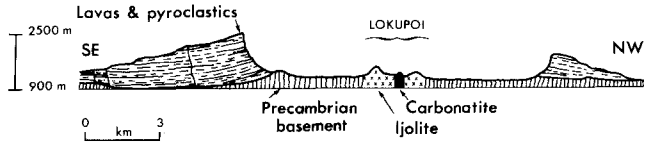

Fig. 2. Cross-section of the Napak carbonatite-nephelinite volcanic complex (after King 1949).

About 1% by volume of the lavas consists of silica-saturated (quartz and albite normative) "andesitic" flows (King 1949), that are chemically similar to mugearites (King and Sutherland 1960). Field evidence suggests that the carbonatite-ijolite core formed largely after extrusion of the lavas, although ijolite fragments in various agglomerate horizons indicate that there may have been more than one period of ijolite formation (King and Sutherland 1960).

In this study, we attempt to: (1) assess the chemical and isotopic evolution of nephelinitic liquids from Napak; (2) characterize the isotopic signature of the sub-continental upper mantle below eastern Uganda.

Analytical methods

Analytical procedures for Nd and Sr are similar to those described in Bell and Blenkinsop (1987). Silicate samples were dissolved in an HF-HNO_3 mixture under pressure for at least 48 h. Carbonate from two carbonatite samples was dissolved using a mixture of HCl-HNO_3. Hand-picked pyroxene phenocryst and nepheline separates were washed in an ultrasonic cleaner using acetone, nanopure water, 2N HCl and then 1N HBr for approximately 30 min. Some whole rock samples were leached using a mixture of cold, dilute HF and 1N HCl for 20 min. Lead was separated in HBr and HCl using a two column anion ion-exchange technique. Details are given in Kwon (1986). The Nd and Sr blanks were about 0.5 ng; those for Pb approximately 1.5 ng. Neodymium and Sr were analysed using a double Re-filament technique, and all isotope ratios were measured on a Finnigan-MAT 261 multicollector solid-source mass spectrometer, operated in the static mode. The Pb samples were run on a single Re filament using silica gel and phosphoric acid.

Petrographic and chemical results

Nephelinites from Napak can be divided into olivine nephelinites, melilite nephelinites and olivine-free nephelinites. The olivine-bearing and olivine-free nephelinites are much more abundant than the melilite nephelinites. The olivine-bearing nephelinites contain phenocrysts of olivine, clinopyroxene and titano-magnetite, while only clinopyroxene and titano-magnetite occur in the olivine-free nephelinites. Compositions of olivine phenocrysts from two of the olivine-bearing nephelinites (samples TL 971 and NP 112) range from Fo_{79} to Fo_{88} (Table 1). Compositions of the clinopyroxene phenocrysts (average size 3 mm) from the olivine-bearing lavas (Table 2) are diopsidic, most have reaction rims (see Table 3), and all are zoned, features that characterize many fractionated nephelinites (Le Bas 1987). Highly zoned and resorbed clinopyroxene phenocrysts also commonly occur in alkalic basalts (Wass 1979) and foidites and basanites (Duda and Schmincke 1985). Clinopyroxenes similar to those from Napak have been documented from other East African alkaline complexes (Le Bas 1987) and from pyroxenites from the Proterozoic Phalaborwa carbonatite complex, South Africa (Eriksson 1989). The increase in acmite content, such as that shown in Fig. 3, characterizes differentiation trends shown by clinopyroxenes from many alkaline melts (Mitchell 1980; Le Bas 1987; Donaldson et al. 1987; Eriksson 1989). Reverse, oscillatory and normal zoning (Table 2, Fig. 3) from different samples, coupled with resorption effects (Simonetti and Bell 1993), suggest a complex crystallization history for the Napak clinopyroxenes. Similar observations have been recorded from clinopyroxenes from Oldoinyo Lengai nephelinites (Donaldson et al. 1987). Diopside phenocrysts also occur in the olivine-free nephelinites (Table 2) but not in the same

Table 1. Average olivine phenocryst microprobe analyses

Sample no.	NP112	NP112	TL971	TL971	TL971
Grain no.	1	2	1	2	3
Number of analyses	6	4	4	4	5
SiO_2	38.52	39.40	38.38	39.75	39.57
MgO	40.57	42.95	40.96	47.48	46.91
FeO	20.85	18.06	19.53	11.15	11.14
MnO	0.29	0.27	0.26	0.20	0.22
NiO	0	0	0	0.08	0.06
CaO	0.31	0.33	0.36	0.38	0.36
Total	100.54	101.00	99.49	99.04	98.26
Fo content	78	81	79	88	88

Olivine and clinopyroxene microprobe analyses were determined using a Cambridge Microscan 5, EDS system. Uncertainties are: major elements ± 2% of quoted value; minor elements 1–5 wt% (± 5%), < 1 wt% (5–10%)

Table 2. Average clinopyroxene microprobe analyses

Sample no.	TL973	TL971	NP101	NP112	TL894	TL690
Type	OB	OB	OB	OB	OF	OF
CORE:						
(Number of analyses)	(8)	(3)	(8)	(12)	(5)	(7)
SiO_2	50.47	50.81	50.78	51.85	50.62	51.08
Al_2O_3	3.39	3.19	3.36	2.82	3.48	2.10
TiO_2	1.27	1.19	1.17	0.96	1.19	0.87
Cr_2O_3	0.16	0.25	0.30	0.32	0.24	0.18
FeO	6.25	6.09	6.28	5.62	6.63	8.89
MgO	14.46	14.60	14.67	15.14	14.34	12.60
MnO	0.07	0.06	0.51	0.03	0.05	0.14
CaO	22.21	23.43	21.82	22.87	22.39	21.37
Na_2O	0.67	0.39	0.65	0.40	0.56	1.16
Total	98.95	100.01	99.54	100.01	99.51	98.39
MIDDLE:						
(Number of analyses)	(5)	(2)	(9)	(11)	(6)	(4)
SiO_2	50.47	50.42	50.93	52.55	50.51	51.20
Al_2O_3	3.18	3.57	3.13	2.24	3.61	2.36
TiO_2	1.19	1.18	1.10	0.81	1.36	0.94
Cr_2O_3	0.20	0.27	0.38	0.46	0.27	0.19
FeO	6.26	6.22	5.79	4.97	6.44	8.32
MgO	14.42	14.44	14.94	15.75	14.27	13.31
MnO	0.01	0.02	0.05	0.04	0.06	0.12
CaO	22.48	23.15	21.84	23.04	22.49	21.83
Na_2O	0.44	0.49	0.59	0.37	0.63	1.17
Total	98.65	99.76	98.75	100.23	99.64	99.44
RIM:						
(Number of analyses)	(5)	(2)	(4)	(11)	(4)	(5)
SiO_2	50.09	51.92	50.94	51.16	49.79	51.2
Al_2O_3	3.46	1.90	3.36	2.97	3.66	1.88
TiO_2	1.25	0.97	1.13	1.22	1.41	0.88
Cr_2O_3	0.16	0.23	0.26	0.44	0.22	0.18
FeO	6.46	5.31	6.28	6.30	6.60	7.66
MgO	14.14	14.98	14.84	14.58	13.83	13.45
MnO	0.0	0.06	0.05	0.04	0.03	0.11
CaO	22.46	23.56	21.67	23.20	22.62	21.91
Na_2O	0.38	0.76	0.74	0.25	0.6	0.76
Total	98.40	99.69	99.27	100.16	98.76	98.03

OB, olivine-bearing nephelinite; OF, olivine-free nephelinite

Table 3. Average compositions of clinopyroxene reaction rims

Sample no.	TL 971	NP 112
Type	OB	OB
Number of analyses	4	8
SiO_2	51.17	51.16
Al_2O_3	1.99	2.04
TiO_2	0.94	1.22
Cr_2O_3	1.14	0.20
FeO	4.64	6.06
MgO	15.29	14.67
MnO	0.04	0.05
CaO	23.51	23.82
Na_2O	0.36	0.05
Total	99.09	99.27

OB, olivine-bearing nephelinite

abundance as the olivine-bearing nephelinites. These are small (< 1 mm) and do not exhibit resorption effects or reaction rims. Figure 3, however, shows that clinopyroxene phenocrysts from sample TL 690, an olivine-free nephelinite, exhibit complex zonation.

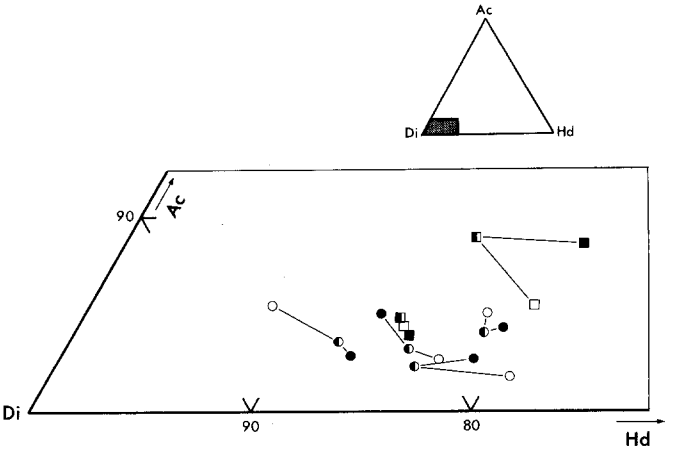

Fig. 3. Individual average core, middle and rim analyses of diopside phenocrysts, from both groups of nephelinites, expressed as *Ac*, acmite (Na cation proportion); *Di*, diopside (Mg cation proportion) and *Hd*, (Fe + Mn cation proportions) ternary end-members. Pyroxene analyses from olivine-bearing nephelinites: *filled circle*, core; *half-filled circle*, middle; and *open cirlce*, rim; pyroxene analyses from olivine-free nephelinites: *filled square*, core; *half-filled square*, middle; and *open square*, rim

Groundmass mineralogy for both groups of nephelinites consists of clinopyroxene, anhedral magnetite, nepheline and a few samples contain minor amounts of biotite, chlorite, zeolites (i.e. natrolite) and secondary calcite (King 1949). Nepheline phenocrysts occur only in one of the samples, a melilite nephelinite (sample TL 944), and nepheline also occurs as prismatic inclusions in some diopside phenocrysts in the olivine-bearing flows (eg. samples TL 973, NP 112).

Whole rock major, trace element analyses and CIPW norms for the nephelinites are given in Table 4a and b. On the basis of their normative mineralogy (Le Bas 1989) the lavas are predominantly melanephelinites (< 5% Ab, < 20% Ne) and nephelinites (< 5% Ab and > 20% Ne). The more primitive nature of the olivine-bearing nephelinites is shown by their higher MgO, Ni, and Cr and lower Al_2O_3, Ba, Sr and Zr contents. In spite of these chemical differences both groups have similar Mg nos. of 61–80, values that can be considered characteristic of primary mantle melts (Roeder and Emslie 1970). Ferrous iron, determined for six samples (NP 100, 101, olivine-bearing nephelinites; TL 690, 894 and NP 102, olivine-free nephelinites; TL 944, melilite nephelinite), show that the olivine-free nephelinites have higher Fe^{3+}/Fe_{total} ratios (0.60–0.71) than the olivine-bearing nephelinites (0.43–0.50). Appropriate ferric/ferrous ratios were assigned to the other nephelinite samples on the basis of their chemical compositions.

Data from the Napak nephelinites are compared in Fig. 4 with differentiation trends (Le Bas 1987) that divide the East African nephelinites into a group I (olivine-rich) and a group II (olivine-poor). On the basis of CaO and MgO contents, the Napak olivine-bearing nephelinites appear to be the least fractionated of the two groups and their data plot at the intersection of the two nephelinite trends shown in Fig. 4. The chemical composition of the Napak olivine-bearing nephelinites (Table 4a) are similar to the group I nephelinites (see Table 1, Le Bas 1987), although they do have somewhat lower Al_2O_3 contents.

Variation diagrams (Figs. 5A to 6) support a cogenetic relationship among the Napak nephelinites, and can be used to interpret the whole range of nephelinites as the product of fractional crystallization

Table 4a. Major and trace element data and CIPW norms

Sample no.	TL944	TL973	NP100	TL971	NP101	NP112
Type	MN	OB	OB	OB	OB	OB
SiO_2	37.15	40.38	42.47	44.36	42.48	43.94
Al_2O_3	11.59	9.44	9.46	8.04	9.93	7.99
TiO_2	2.71	2.52	2.08	1.92	2.26	2.07
Fe_2O_3	7.36	7.91	5.86	7.38	7.06	6.67
FeO	6.47	5.37	7.80	5.01	7.03	6.66
MgO	5.69	10.32	9.95	11.35	10.30	11.98
MnO	0.24	0.18	0.20	0.19	0.2	0.17
CaO	13.98	14.25	14.57	15.64	14.04	14.86
Na_2O	4.49	3.46	4.67	3.32	4.03	3.22
K_2O	3.62	2.56	2.50	1.64	2.16	1.43
P_2O_5	0.73	0.36	0.43	0.41	0.47	0.24
S	0.01	0.0	0.01	0.01	0.01	0.01
H_2O	1.49	0.56	0.49	–	0.46	–
LOI	4.87	0.82	0.51	–	0.95	–
Total	100.40	98.13	101.00	99.27	101.38	99.24
Mg no.[a]	61	77	69	80	72	76
Ba	1180	888	840	669	796	540
Cr	24	164	341	534	183	475
Zr	157	87	119	98	117	81
Sr	1188	415	690	577	683	439
Rb	105	75	54	38	55	34
Y	27	17	22	19	21	16
Nb	110	55	66	48	63	39
Zn	107	76	94	81	93	71
Ni	31	61	104	105	94	142
V	218	210	201	216	130	251
CIPW norms						
Or	0.0	0.0	0.0	2.8	0.0	5.9
Ab	0.0	0.0	0.0	0.0	0.0	0.0
An	0.8	2.7	0.0	2.2	2.6	3.1
Lc	16.8	11.9	11.6	5.4	10.0	2.0
Ne	20.6	15.9	18.8	15.2	18.5	14.8
Ac	0.0	0.0	4.2	0.0	0.0	0.0
Di	25.5	40.3	34.3	57.0	45.9	54.0
Ol	2.5	5.0	11.5	1.5	5.5	3.5
Cs	9.6	4.5	8.4	0.0	2.0	0.0
Mt	10.7	10.6	6.4	10.7	10.2	11.5
Cm	0.0	0.0	0.1	0.1	0.0	0.1
Hm	0.0	0.6	0.0	0.0	0.0	0.0
Il	5.2	4.8	4.0	3.7	4.3	3.9
Ap	1.7	0.9	1.0	1.0	1.1	0.6

Data obtained by XRF. The relative precision of the major element oxide analyses, with the exceptions of Na_2O, P_2O_5, MnO and S, is equal to or less than 3% of determined value; the precision of Na_2O, P_2O_5, MnO and S is ± 10%. Relative precision of the trace element results (ppm) is ± 10% for all the elements except Y (± 50%). MN, melilite nephelinite; OB, olivine-bearing nephelinite; (- -), not analysed

[a] Mg no. = molar MgO/(molar MgO + molar FeO)

Table 4b. Major and trace element analyses and CIPW norms of olivine-free nephelinites and average commposition of mafic granulites

Sample no.	NP102	TL894	NP111	TL931	TL690	Granulite[b]
SiO_2	42.50	42.36	40.37	42.96	46.36	51.72
Al_2O_3	12.62	12.37	12.68	10.74	15.66	18.56
TiO_2	2.48	2.44	2.31	1.97	1.34	0.43
Fe_2O_3	8.76	8.83	9.05	9.30	7.57	1.61
FeO	5.89	5.98	4.88	3.99	3.09	3.24
MgO	6.10	6.19	4.94	8.05	3.94	6.01
MnO	0.23	0.24	0.24	0.22	0.21	0.08
CaO	11.81	12.56	13.61	14.69	9.41	10.39
Na_2O	3.83	5.06	5.72	3.72	4.94	4.05
K_2O	1.83	1.79	2.95	1.94	1.96	0.95
P_2O_5	0.74	0.96	1.08	0.77	0.30	0.10
S	0.0	0.01	0.0	0.0	0.0	0.0
H_2O	1.83	1.28	1.14	1.03	2.16	0.63
LOI	2.63	1.54	2.48	1.67	5.35	1.73
Total	101.25	101.61	101.45	101.05	102.29	99.71
Mg no.[a]	66	65	76	79	69	76
Ba	1019	492	741	1252	1090	328
Cr	41	48	12	205	47	273
Zr	154	161	199	177	144	228
Sr	1076	857	1156	1405	1528	1338
Rb	41	46	58	38	67	22
Y	26	27	31	28	24	4
Nb	77	83	106	87	64	n.r.
Zn	116	124	141	117	125	n.r
Ni	32	40	26	71	50	198
V	178	227	208	183	138	n.r.
CIPW norms						
Or	10.8	10.6	5.3	10.8	11.6	5.6
Ab	10.2	6.5	0.0	0.0	22.7	33.5
An	11.9	5.8	0.2	6.9	14.8	29.7
Lc	0.0	0.0	9.5	0.5	0.0	0.0
Ne	12.0	19.7	26.2	17.1	10.4	0.4
Ac	0.0	0.0	0.0	0.0	0.0	0.0
Di	32.9	33.5	26.6	44.0	21.3	9.9
Ol	0.0	0.0	0.0	0.0	0.0	7.6
Cs	0.0	0.0	0.0	0.0	0.0	0.0
Mt	11.8	12.8	11.5	11.0	6.8	2.4
Cm	0.0	0.0	0.0	0.0	0.0	0.0
Hm	0.2	0.0	0.0	0.0	2.9	0.0
Il	4.7	4.6	4.4	3.7	2.5	0.8
Ap	1.8	2.3	2.6	1.8	0.7	0.2

See footnotes of Table 4a; n.r., not reported

[b] average analysis of mafic granulite, based on three xenolith samples from the Lashaine tuff cone, Tanzania (Dawson 1977)

of a single parental melt. Element variation diagrams (Fig. 5A–C) show that clinopyroxene and titanomagnetite along with olivine, could have controlled the compositional evolution of the parental melt. In the Pearce element ratio diagram (Pearce 1990) shown in Fig. 6 a data set with a slope of 1 would be consistent with clinopyroxene and olivine fractionation in a closed system. With the exception of sample TL 690, the data from both groups of nephelinites, and in particular the data from the olivine-bearing lavas, define a linear array with a slope of approximately 0.9. Support for olivine and pyroxene fractionation is also given by other plots (e.g. 0.5 $(MgO + FeO)/TiO_2$ vs SiO_2/TiO_2; $2CaO/TiO_2$ vs SiO_2/TiO_2), suggesting that both minerals were simultaneously crystallizing, an interpretation that is consistent with petrographic observation.

The variation diagrams bring out the following features: (1) the Napak nephelinites may be related to one parental magma; (2) the olivine-bearing nephelinites are chemically the most primitive; (3) melt fractionation was partly controlled by olivine and clinopyroxene. The uniformly high Mg numbers from both groups of Napak nephelinites, however, is inconsistent with closed-system olivine and clinopyroxene fractionation of a single magma.

Isotopic results

The Nd, Pb and Sr isotopic ratios are shown in Table 5 and all are considered initial ratios because of the relatively young age of the complex. The Nd and Sr isotopic data, plotted in Fig. 7, form a curvilinear array that extends from the upper-left (depleted) to the lower-left quadrant of the anticorrelation plot. Anchored well inside the depleted quadrant, the isotopic data from two carbonatites and two nephelinites (TL 944 melilite nephelinite; TL 973 olivine-bearing nephelinite) are similar to those from other young Ugandan carbonatites associated with the Eastern rift (Bell and Blenkinsop 1987), used to define one extreme of the East African Carbonatite Line (EACL, Bell and Blenkisop 1987). The data from the two carbonatite samples are similar to those obtained by Nelson et al. (1988) from Napak. Isotopic data from the remaining nine samples from Napak approximate a hyperbola, with the

olivine-bearing nephelinites showing the highest $^{143}Nd/^{144}Nd$ ratios and lowest $^{87}Sr/^{86}Sr$ ratios. Compared to the relatively uniform isotopic composition of silicate lavas from other East African carbonatite complexes, such as Shombole (Fig. 7; Bell and Peterson 1991), the isotopic variation shown by the Napak nephelinites is relatively large. The range in Nd and Sr of the Napak isotopic ratios span almost the entire range of values observed from several East African cabonatite complexes (Bell and Blenkinsop 1987).

Six pyroxene phenocryst populations from the olivine-bearing nephelinites have isotopic ratios that, in most cases, are significantly different from those of their enclosing lavas. Most have much lower Pb and Sr isotopic ratios, yet Nd isotopic ratios (Figs. 7, 8A, B) the same as or higher than their whole rocks (Simonetti and Bell 1993). Leaching experiments on three whole rock olivine-bearing nephelinite samples were used to assess the role, if any, of groundwater interaction in producing the intra-sample isotopic differences between phenocrysts and host lavas. Typical late-stage alteration by Nd-depleted and Sr-enriched groundwaters would shift the original isotopic composition of a sample horizontally to the right on a Nd-Sr plot, such as Fig. 7. The results of the leaching experiments (Table 5; Fig. 7) indicate that any groundwater interaction with the nephelinites was limited, and that the influence on the isotopic ratios was slight. The relatively fresh and unaltered nature of the nephelinite samples in thin section add support to this conclusion. Disequilibrium crystallization has also been documented for clinopyroxene phenocrysts from phonolites from the Lacher See volcanics, East Eifel (Wörner et al. 1984), and attributed to either change in melt composition by assimilation, or late-stage fluid exchange between melt and wall rock.

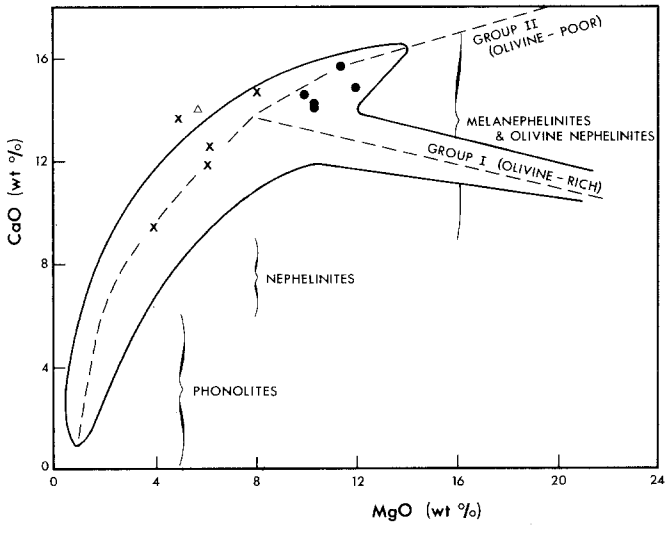

Fig. 4. Plot of CaO wt% versus MgO wt% (Le Bas 1987) for Napak whole rock nephelinite analyses. *Filled circles*, olivine-bearing; *Xs*, olivine-free; *open triangle*, melilite nephelinite

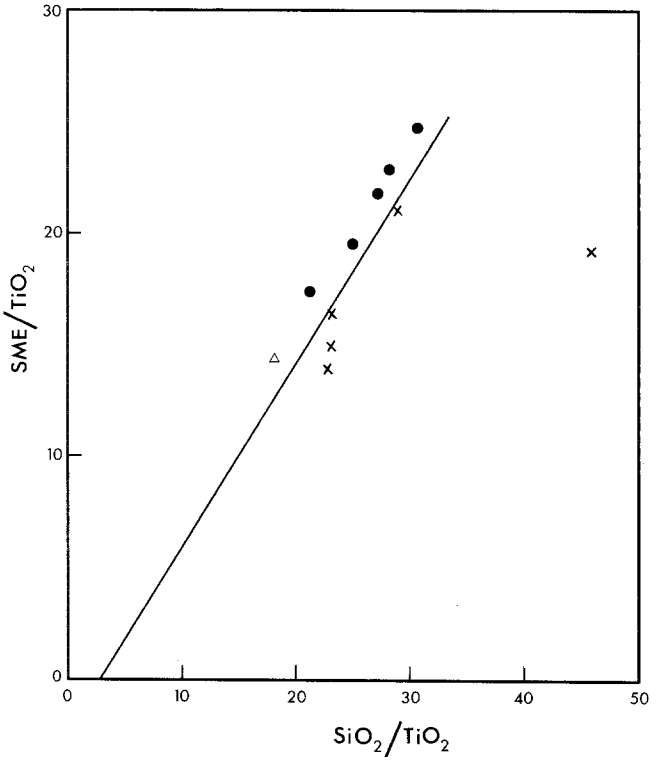

Fig. 6. *SME* = molar [1.5 CaO + 0.5(FeO + MgO)] (Pearce 1990). Symbols as in Fig. 4. Excluding the data from an olivine-free nephelinite sample, the slope of the line is 0.85 ± 0.04

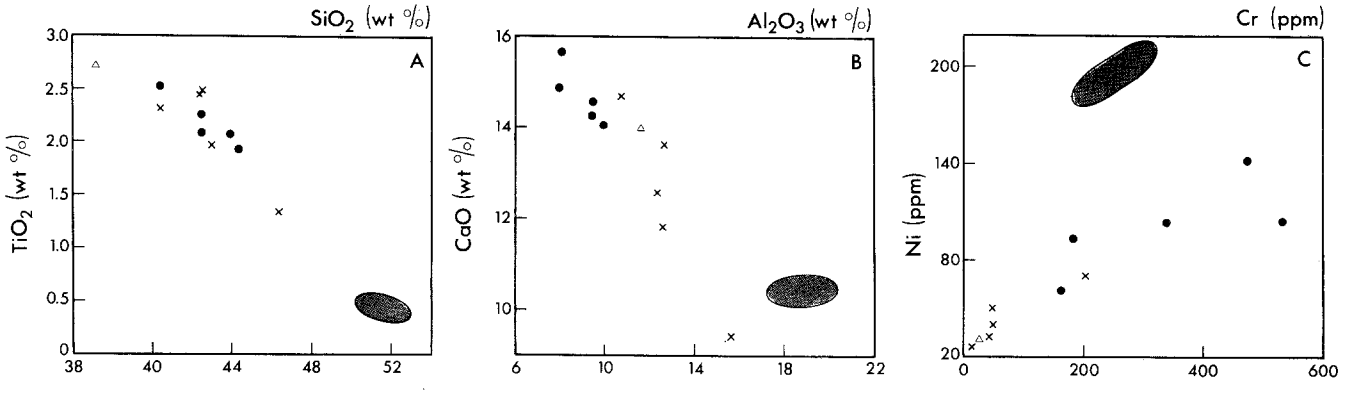

Fig. 5A-C. Variation diagrams for Napak whole rock nephelinite data. **A** SiO_2 (wt%) versus TiO_2 (wt%); **B** Al_2O_3 (wt%) versus CaO (wt%); **C** Cr (ppm) versus Ni (ppm). Symbols as in Fig. 4. Mafic granulite field, shaded, outlined from data from Dawson (1977)

Table 5. Nd, Pb and Sr whole rock and mineral data from Napak

Sample	Sr (ppm)	$^{143}Nd/^{144}Nd$ (atomic)	$^{87}Sr/^{86}Sr$ (atomic)	$^{206}Pb/^{204}Pb$	$^{207}Pb/^{204}Pb$	$^{208}Pb/^{204}Pb$
Melilite nephelinite						
TL 944	1188	0.51275	0.70327	21.52	15.85	40.81
Olivine nephelinites						
TL 971	577	0.51250	0.70359	20.44	15.81	40.31
TL 973	415	0.51274	0.70342	21.37	15.89	40.78
TL 973 Leachate		0.51279	0.70344			
NP 100	690	0.51259	0.70330	20.53	15.77	40.10
NP 101	683	0.51248	0.70342	19.48	15.73	39.21
NP 101 Leachate		0.51251	0.70357			
NP 112	439	0.51243	0.70351	19.78	15.71	39.56
NP 112 Leachate		0.51248	0.70351			
Olivine-free nephelinites						
TL 690	1528	0.51223	0.70435	20.18	15.81	39.91
TL 894	857	0.51243	0.70381	19.84	15.74	39.88
TL 931	1405	0.51238	0.70442	19.29	15.73	39.88
NP 102	1076	0.51238	0.70351	19.63	15.76	39.70
NP 111	1156	0.51238	0.70403	19.48	15.69	39.70
Carbonatites						
BM 1990 P7 (181)	3959	0.51283	0.70323	20.40	15.81	40.46
BM 1990 P7 (198)	4984	0.51283	0.70323	20.47	15.75	40.21
Ijolite (NP 110)						
Nepheline	135	0.51264	0.70549	20.62	15.82	40.31
Pyroxene	290	0.51266	0.70491	20.85	15.84	40.38

Isotope results normalized to $^{146}Nd/^{144}Nd = 0.7219$ and $^{86}Sr/^{88}Sr = 0.1194$. NBS 987 Sr standard = 0.71025 ± 0.00002; La Jolla Nd standard = 0.51186 ± 0.00002; and BCR-1 $^{143}Nd/^{144}Nd = 0.51266 \pm 0.00002$. Uncertainties are given at the 2 sigma level. Sr abundances, with the exception of the two carbonatite samples and ijolite mineral separates (determined by isotope dilution), were determined by XRF analysis. Reproducibility of Pb isotopic ratios is 0.1%. An average fractionation factor of 0.1% per mass unit was applied to all measured ratios based on analyses of NBS 982

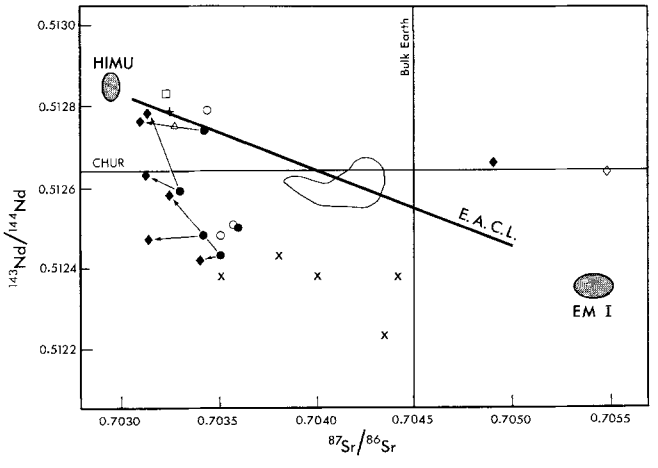

Fig. 7. E.A.C.L. from Bell and Blenkinsop (1987), isotopic composition of HIMU and EM I from Hart (1988). Symbols: *filled diamonds*, diopside phenocrysts from olivine-bearing nephelinites and ijolite; *open diamond*, nepheline from central ijolite; *open circles*, olivine-bearing nephelinite whole rock leachates; *open square*, 2 Napak carbonatite samples analysed in this study; +, Napak carbonatite analysis (Nelson et al. 1988); other symbols as in Fig. 4. *Tie-lines* join diopside phenocryst with corresponding whole rock analysis (Simonetti and Bell 1993). *Enclosed area* marks the distribution of the data from Shombole (Bell and Peterson 1991)

The Pb isotopic results of the whole rocks and two mineral separates from the central ijolite, the supposed plutonic equivalent of the nephelinites, are presented in Table 5 and plotted in Fig. 8A and B. The Pb isotopic ratios plot to the right of both the geochron and the Stacey-Kramers (1975) growth curve. The two nephelinites with the most radiogenic Pb ratios (TL 944; TL 973) have the most depleted Nd and Sr isotopic signatures and have Nd, Sr and Pb isotopic ratios similar to those of the two Napak carbonatites. The variation in Pb isotopic ratios from the Napak lavas is similar to that found for all data so far collected from other East African carbonatite centres (Allègre et al. 1979; Grünenfelder et al. 1986).

The near-linear arrays of the data in plots of $^{207}Pb/^{204}Pb$ versus $^{206}Pb/^{204}Pb$ and $^{208}Pb/^{204}Pb$ versus $^{206}Pb/^{204}Pb$, including the data from pyroxene phenocrysts from the olivine-bearing nephelinites, has a slope of about 0.10. The higher $^{208}Pb/^{204}Pb$ ratios for a given $^{206}Pb/^{204}Pb$ ratio (Fig. 8B) for the olivine-free nephelinites suggests possible interaction with, or derivation from a time integrated, Th-enriched reservoir.

The Nd and Sr isotope ratios of pyroxenes and nephelines from a coarse-grained ijolite (NP 110) are significantly more radiogenic, in terms of Sr, than any of the other samples from Napak. Although, the Sr isotopic

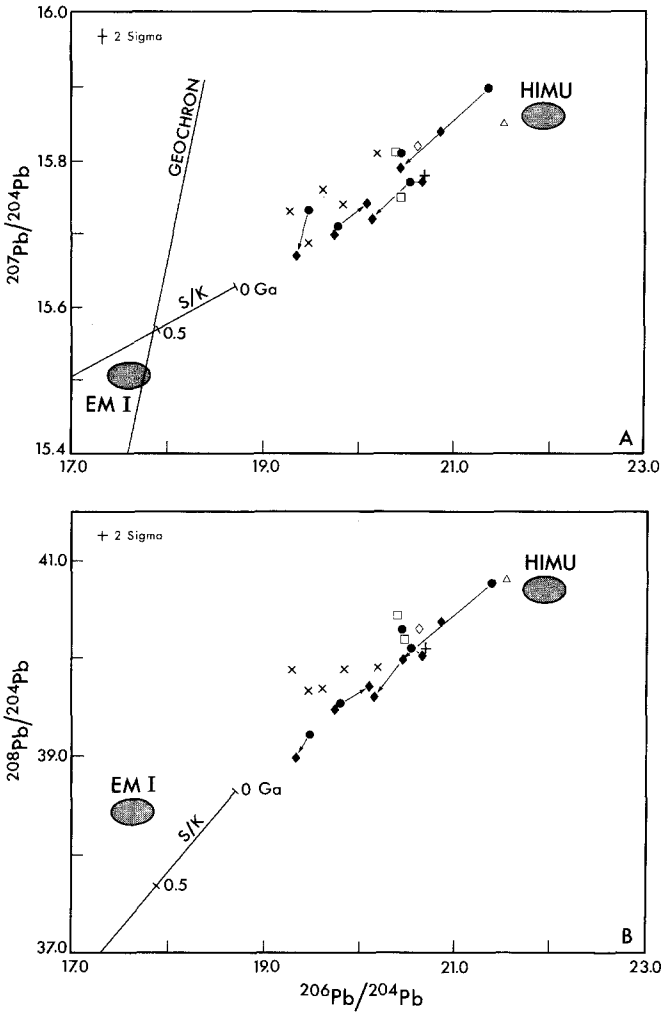

Fig. 8A,B. HIMU and EM I mantle components are from Hart (1988). *S/K*, Stacey-Kramers growth cruve (Stacey and Kramers 1975). Symbols as in Fig. 4. *Tie-lines* join diopside phenocryst with corresponding whole rock analysis (Simonetti and Bell 1993)

ratios of the nepheline are more radiogenic than the coexisting pyroxene, their Nd isotopic compositions are identical. The Pb isotopic data, however, plot along the trend defined by the Napak pyroxene and associated whole rock data, and are among the most radiogenic of the Pb analyses.

The large Nd, Pb, and Sr isotopic variations of the Napak samples are best attributed to open-system behaviour. The isotopic disequilibrium demonstrated between the clinopyroxene phenocrysts and their host olivine-bearing nephelinite lavas are consistent with this model. The clinopyroxenes clearly did not crystallize from their host liquid (Simonetti and Bell 1993), and such isotopic disequilibrium may be attributed to isotopic shifts in the host lava during clinopyroxene crystallization caused by: (1) assimilation of crustal material; (2) mixing of melts generated from an isotopically heterogeneous source.

Discussion

Most of the Nd and Sr isotopic data from Napak plot in the lower-left quadrant of the Nd-Sr plot, a feature that is inconsistent with the known chemical behaviour of the two parent nuclides, ^{147}Sm and ^{87}Rb. Data that fall in the lower-left quadrant include some from metasomatized mantle xenoliths (Menzies and Murthy 1980), inclusions in diamonds (Richardson et al. 1984), mafic granulites (Cohen et al. 1984), some continental basalts (Carter et al. 1978) and some phonolites (Bell and Peterson 1991). Isotopic data from mantle-derived rocks that lie to the left of the "mantle array" (Fig. 7) are difficult to explain, but explanations include influx of a vapour phase into a mantle source (Barriero 1983; Menzies and Wass 1983; Meen et al. 1989), special mantle sources (Menzies and Murthy 1980), or mixing of a mantle-derived melt with amphibolites or granulites (Carter et al. 1978; Bell and Peterson 1991).

Large variations in Sr isotope ratios, similar to that shown in Fig. 7, from some Napak nephelinites, were earlier attributed by Bell and Powell (1970) to open-system behaviour, involving crustal assimilation. The array, however, can be interpreted in other ways including assimilation combined with fractional crystallization, or mixing of distinct mantle melts. Each of these models will be discussed in turn.

Crustal assimilation. Generation of the Napak trend by mixing would have to involve one component with a HIMU isotope signature, such as a mantle-derived melt, and a second end-member with Sr and Nd ratios that fall in the lower-left or lower-right hand (enriched) quadrants (Fig. 7). One possible end-member that plots in the lower-left quadrant is mafic granulite (Cohen et al, 1984), found as xenoliths in ankaramite scoria and carbonatitic tuffs from the Lashaine tuff cone, Tanzania (Jones et al. 1983). These mafic granulites are garnet-plagioclase clinopyroxenites corresponding in bulk chemical composition to olivine normative alkali gabbros (Cohen et al. 1984) and thought to have equilibrated at a temperature between 900 and 950°C and a pressure of 13 to 15 kbar. The average chemical composition of the mafic granulite is given in Table 4b. Compared to the Napak nephelinites, the mafic granulites have similar Na_2O contents, only slightly higher SiO_2, Al_2O_3 contents, and somewhat lower total Fe, MgO, TiO_2, K_2O, and CaO contents. That the mafic granulite field, shown in Fig. 5A and B, always plots at one extreme of the trends is consistent with mafic granulites being one of the end-members in the mixing array.

Isotopic evidence for binary mixing is shown by the positive correlation between $^{87}Sr/^{86}Sr$ and total Sr (Fig. 9A). One end-member has a high $^{87}Sr/^{86}Sr$ ratio (> 0.7044) and high Sr content (1500 ppm), (cf. the mafic granulite data given by Cohen et al. 1984), while the other has a low $^{87}Sr/^{86}Sr$ (< 0.7033) and low Sr (< 400 ppm) content, similar to the most primitive of the olivine-bearing nephelinites from Napak. A negative correlation between $^{87}Sr/^{86}Sr$ and Rb/Sr (Fig. 9B), is also consistent with simple binary mixing between mafic granulites and a nephelinite magma. Although simple binary mixing between a parental nephelinite magma and mafic granulite can explain some of the data, such as that shown in Fig. 9A and B, it fails, on the basis of the Nd and Sr isotope data, to generate a hyperbola similar to the one shown in the anticorrelation plot (Fig. 7). Other problems with any

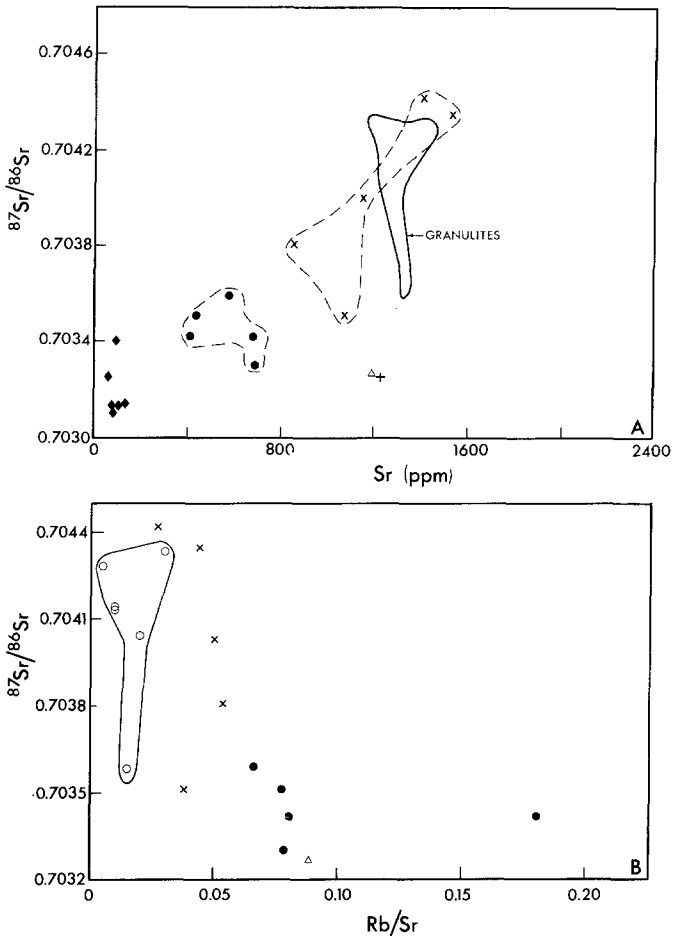

Fig. 9. A $^{87}Sr/^{86}Sr$ versus Sr (ppm). **B** $^{87}Sr/^{86}Sr$ versus Rb/Sr. Granulite field and data, *open circles*, from Cohen et al. (1984). Other symbols as in Figs. 4 and 7

model that involves assimilation of mafic granulites is the retention of the nephelinitic character of the melts, and the thermal budget required for bulk assimilation.

Assimilation combined with fractional crystallization. An alternative model to simple binary mixing is assimilation and fractional crystallization (DePaolo 1981). Sample TL 973, an olivine-bearing nephelinite has the most primitive isotope composition ($^{143}Nd/^{144}Nd = 0.51274$, $^{87}Sr/^{86}Sr = 0.70342$) and is considered to be the primary magma (Sr = 415 ppm), and the average Lashaine granulite (Cohen et al. 1984) the contaminant (average $^{143}Nd/^{144}Nd = 0.5120$, $^{87}Sr/^{86}Sr = 0.7042$, Sr = 1400 ppm). A Nd content of 48 ppm, based on three reported Nd values for Napak nephelinites (Le Bas 1987), was used as the initial Nd content of the magma, and an average Nd content of 4 ppm for the Lashaine granulites. The AFC model is partly successful, but only if a large amount of contaminant ($r > 0.6$, r = mass of assimilant/mass of original magma) is used and unrealistic partition coefficients for Nd (i.e. greater than one) are assumed. Other problems with the AFC model include: (1) the lack of agreement between calculated and observed Nd and Sr abundances; (2) knowledge of appropriate partition coefficients for diopside and nepheline in nephelinites; (3) the more radiogenic $^{208}Pb/^{204}Pb$ ratios from the olivine-free nephelinites; (4) the consistent nephelinitic nature and high Mg numbers of even the most "contaminated" lavas.

Mixing of different mantle melts. Magma mixing has been invoked to explain similar textural and chemical features in clinopyroxenes from other continental alkalic centres. For example, Duda and Schmincke (1985) attributed the variation in chemical compositions in pyroxenes from the West Eifel volcanics to polybaric crystallization and mixing between an earlier-differentiated magma and a later-derived primitive mantle melt.

Two component mixing has also been proposed to explain the variations in isotopic data from recent East African carbonatite complexes (Bell and Blenkinsop 1987). Isotopic results define the EACL, a Nd-Sr isotopic array defined mainly by young (< 30 Ma) carbonatites from Kenya, Tanzania and Uganda, similar in slope to the "Lo-Nd" array of Hart et al. (1986). The EACL may therefore represent cabonatites derived from a mixture of HIMU and EM I mantle components (Bell and Blenkinsop 1987), the two end-members of the "Lo-Nd" array (Hart et al. 1986). The linear nature of the EACL (Fig. 7) requires that the Sr/Nd ratio in both the HIMU and EM I end-members is similar.

The data from Napak (Fig. 7) are inconsistent with mixing of melts derived from pure HIMU and pure EM I since they form a hyperbola, rather than a straight line, indicating that the Sr/Nd ratios for the two end-members can not be the same. Because the nephelinitic magmas are derived from a metasomatized mantle, it is always possible that the Sr/Nd ratio of one of the end-members could have been perturbed during metasomatic activity.

If mixing has taken place between mantle melts beneath Napak, the relatively high Mg numbers of almost all nephelinites suggest that both were relatively unfractionated. The clustering of the data, into what may appear to be distinct groups (Fig. 9A), may be an argument for the possible mixing of at least two primary nephelinite magmas.

Isotopic evidence for such a model can be inferred from the Pb isotopic data, which show similar isotopic patterns to other mantle-derived rocks. The slope of the $^{207}Pb/^{204}Pb$–$^{206}Pb/^{204}Pb$ array of the pyroxene and olivine-bearing nephelinite data (Fig. 8A) is similar to that of the East African carbonatite complexes (Grünenfelder et al. 1986), the oceanic regression line (Tatsumoto 1978), and a Pb isotopic array defined by clinopyroxenes from mantle xenoliths from western Uganda (Davies and Lloyd 1991). The Pb isotopic data suggest mixing, in both continental and oceanic areas, between similar mantle end-members, although mixing between a HIMU component, and mafic granulites would produce a similar slope. On the basis of Pb isotopes alone it is difficult to distinguish mafic granulites from pure EMI. However, the Sr and Nd isotopic signatures of the nephelinites rule out interaction between melts derived from HIMU and pure EMI.

Evidence for open-system behaviour has also been provided by Simonetti and Bell (1993). Intra-sample pyroxene populations from samples NP 100 and NP 112 have different isotopic (Figs. 7, 8A, B) and chemical compositions, suggesting that the pyroxene populations did not crystallize from the same melt, nor did they precipitate

from the melt that hosts them. The fact that the slope (about 0.10) of the $^{207}Pb/^{204}Pb$ versus $^{206}Pb/^{204}Pb$ linear array from Napak is similar to the regression line based on oceanic basalts (Tatsumoto 1978), and a Pb isotopic array defined by clinopyroxenes from mantle xenoliths from western Uganda (Davies and Lloyd 1991), would tend to support a model that involves the mixing of distinct mantle partial melts from an isotopically heterogeneous mantle source region.

On the basis of the evidence available to us it is difficult to preferentially favour any one of the three models. No matter which model is chosen, consideration should be given to the following: (1) the isotopic data have shown that the system was chemically open; (2) both the petrography and some of the chemical data favour olivine and pyroxene fractionation.

The relationship between the central ijolite and the nephelinites, the supposed volcanic equivalents, is not as yet clear. On the basis of the Nd and Sr isotopic results from the pyroxene and nepheline populations of sample NP 110 (Table 5), the ijolite seems to have had an evolutionary history quite different to that of the nephelinites. Although the Pb isotopic data given in Fig. 8A and B, for both extrusive and intrusive rocks at Napak, lie along the same linear array, there are significant differences in the Nd and Sr isotopic data. The Sr isotopic ratios for both the nepheline and the pyroxene separates from the ijolite are much more radiogenic than any of the other ratios measured from Napak, and their Nd isotopic compositions are similar to bulk Earth. On the basis of only one sample it is difficult to reconcile the ijolite and nephelinite data, but the more radiogenic Sr for the plutonic rock suggests involvement with a more enriched source.

Conclusions

The Nd, Pb and Sr isotopic variations from the Napak complex alone span almost the entire range of isotopic data obtained from all the East African nephelinite-carbonatite complexes studied to date (Allègre et al. 1979; Grünenfelder et al. 1986; Bell and Blenkinsop 1987), and caution against using a single analysis from an eruptive centre to characterize the mantle source. The major and trace element data along with the isotopic data from the Napak nephelinites are compatible with a binary mixing model coupled with fractionation of both olivine and clinopyroxene. The isotopic data from the Napak nephelinites reflect a complicated magma system that involved open-system fractionation of olivine and clinopyroxene at either mantle or lower crustal levels. The textures, chemical variations and isotopic disequilibrium exhibited by the Napak clinopyroxene phenocrysts support crystal fractionation of a melt undergoing continuous isotopic change. Such changes can be attributed to assimilation of mafic granulites or mixing of mantle melts derived from a heterogeneous source. Although some of the major and trace element data from the whole rock nephelinites can be attributed to the crystal fractionation of a single parental magma, the large isotopic variations are clearly inconsistent with this being the sole mechanism.

Acknowledgements. We would like to thank J. W. Card for his critical comments on the manuscript and for his assistance in drafting diagrams, and Peter Jones for help in obtaining the probe data. A. R. Woolley kindly provided the two carbonatite samples. One of us (K. B.) would like to thank the Geological Survey of Uganda for donating samples from their reference collection, and providing logistical support many years ago. NSERC provided monies to partly support this project. Thoughtful reviews from P. J. Patchett, G. Wörner and an anonymous reviewer, were much appreciated, and their comments greatly improved the manuscript.

References

Allègre CJ, Ben Othman D, Polve M, Richard P (1979) The Nd and Sr isotopic correlation in mantle materials and geodynamic consequences. Earth Planet Sci Lett Int 19:293–306

Allen JC, Boettcher AL, Marland G (1975) Amphiboles in andesite and basalt. I. Stability as a function of P-T-f_{O_2}. Am Mineral 60:1069–1085

Baker BH, Williams LAJ, Miller JA, Fitch FJ (1971) Sequence and geochronology of the Kenya rift volcanics. Tectonophysics 11:191–215

Barriero B (1983) An isotopic study of Westland dike swarm, South Island, New Zealand. Carnegie Inst Washington Yearb 82:471–475

Bell K, Blenkinsop J (1987) Nd and Sr isotopic compositions of East African carbonatites: implications for mantle heterogeneity. Geology 15:99–102

Bell K, Peterson TD (1991) Nd and Sr isotope systematics of Shombole volcano, East Africa, and the links between nephelinites, phonolites, and carbonatites. Geology 19:582–585

Bell K, Powell JL (1970) Strontium isotopic studies of alkalic rocks: the alkalic complexes of eastern Uganda. Bull Geol Soc Am 81:3481–3490

Bishop WW (1958) Miocene mammalia from the Napak volcanics, Karamoja, Uganda. Nature 182:1480–1482

Bishop WW, Miller JA, Fitch FJ (1969) New potassium – argon age determinations relevant to the Miocene fossil mammal sequence in East Africa. Am J Sci 267:669–699

Brey GP (1978) Origin of olivine melilitite – chemical and experimental constraints. J Volcano Geothermal Res 3:61–88

Brey GP, Green DH (1977) Systematic study of liquidus phase relations in olivine melilitite-H_2O + CO_2 at high pressure and the petrogenesis of an olivine melilitite magma. Contrib Mineral Petrol 61:141–162

Bultitude RJ, Green DH (1968) Experimental study at high pressures on the origin of olivine nephelinite and olivine melilite nephelinite magmas. Earth Planet Sci Lett 3:325–327

Bultitude RJ, Green DH (1971) Experimental study of crystal-liquid relationships at high pressures in olivine nephelinite and basanite compositions. J Petrol 12:121–147

Cahen L, Snelling NJ, Delhal J, Vail JR (1984) Phanerozoic anorogenic igneous activity in Africa. In: The geochronology and evolution of Africa. Clarendon Press, Oxford, pp 375–415

Carter SR, Evensen NM, Hamilton PJ, O'Nions RK (1978) Neodymium and strontium isotope evidence for crustal contamination of continental volcanics. Science 202:743–746

Cohen RS, O'Nions RK, Dawson JB (1984) Isotope geochemistry of xenoliths from East Africa: implications for development of mantle reservoirs and their interaction. Earth Planet Sci Lett 68:209–220

Davies GR, Lloyd FE (1991) Pb-Sr-Nd isotope and trace element data bearing on the origin of the potassic subcontinental lithosphere beneath south-west Uganda. In: Kampunzu AB, Lubala RT (eds) Magmatism in extensional structural settings: the Phanerozoic African plate. Springer, Berlin Heidelberg New York, pp 784–794

Dawson JB (1977) Sub-cratonic crust and upper mantle models based on the xenolithic suites in kimberlite and nephelinitic diatremes. J Geol Soc London 134:173–184

DePaolo DJ (1981) Trace element and isotopic effects of combined wall-rock assimilation and fractional crystallization. Earth Planet Sci Lett 53:189–202

Donaldson CH, Dawson JB, Kanaris-Sotiriou R, Batchelor RA, Walsh JN (1987) The silicate lavas of Oldoinyo Lengai, Tanzania. Neues Jahrb Mineral Abh 156:247–279

Duda A, Schmincke H-U (1985) Polybaric differentiation of alkali basaltic magmas: evidence from green-core clinopyroxenes (Eifel, FRG). Contrib Mineral Petrol 91:340–354

Eggler DH (1989) Carbonatites, primary melts, and mantle dynamics. In: Bell K (ed) Carbonatites: genesis and evolution. Unwin Hyman, London, pp 561–579

Eriksson SC (1989) Phalaborwa: a saga of magmatism, metasomatism and miscibility. In: Bell K (ed) Carbonatites: genesis and evolution. Unwin Hyman, London, pp 221–254

Frey FA, Green DH, Roy GD (1978) Integrated models of basalt petrogenesis: a study of quartz tholeiites to olivine melilitites from southeastern Australia utilizing geochemical and experimental petrological data. J Petrol 19:463–513

Grünenfelder MH, Tilton GR, Bell K, Blenkinsop J (1986) Lead and strontium isotope relationships in the Oka carbonatite complex, Quebec. Geochim Cosmochim Acta 50:461–468

Hart SR (1988) Heterogeneous mantle domains: signatures, genesis and mixing chronologies. Earth Planet Sci Lett 90: 273–296

Hart SR, Gerlach DC, White WM (1986) A possible new Sr-Nd-Pb mantle array and consequences for mantle mixing. Geochim Cosmochim Acta 50:1551–1557

Jones AP, Smith JV, Hansen EC, Dawson JB (1983) Metamorphism, partial melting and K-metasomatism of garnet-scapolite-kyanite granulite xenoliths from Lashaine, Tanzania. J Geol 91:143–165

King BC (1949) The Napak area of southern Karamoja, Uganda. Mem Geol Surv Uganda 5

King BC, Sutherland DS (1960) Alkaline rocks of eastern and southern Africa. Sci Prog London 48:298–321

Kwon ST (1986) Pb-Sr-Nd isotope study of the 100 to 2700 Ma old alkalic rock-carbonatite complexes in the Canadian Shield: inferences on the geochemical and strucutral evolution of the mantle. PhD thesis, Univ California, Santa Barbara, California, USA

Le Bas MJ (1987) Nephelinites and carbonatites. In: Fitton JG, Upton BGJ (eds) Alkaline igneous rocks. Spec Publ Geol Soc 30:53–83

Le Bas MJ (1989) Nephelinitic and basanitic rocks. J Petrol 30:1299–1312

Lloyd FE, Bailey DK (1975) Light element metasomatism of the continental mantle: the evidence and the consequences. Phys Chem Earth 9:389–416

Meen JK, Ayers JC, Fregeau EJ (1989) A model of mantle metasomatism by carbonated alkaline melts: trace-element and isotopic compositions of mantle source regions of carbonatite and other continental igneous rocks. In: Bell K (ed) Carbonatites: genesis and evolution. Unwin Hyman, London, pp 464–499

Menzies M, Murthy VR (1980) Nd and Sr isotope geochemistry of hydrous mantle nodules and their host alkali basalts: implications for local heterogeneities in metasomatically veined mantle. Earth Planet Sci Lett 46:323–334

Menzies MA, Wass S (1983) CO_2-rich mantle below eastern Australia: REE, Sr and Nd isotopic study of Cenozoic alkaline magmas and apatite-rich xenoliths, southern Highlands Province, New South Wales, Australia. Earth Planet Sci Lett 65:287–302

Merrill RB, Wyllie PJ (1975) Kaersutite and kaersutite eclogite from Kakanui, New Zealand–water-excess and water-deficient melting relations to 30 kilobars. Bull Geol Soc Am 86:555–570

Mitchell RH (1980) Pyroxenes of the Fen alkaline complex, Norway. Am Mineral 65:45–54

Nelson DR, Chivas AR, Chappell BW, McCulloch MT (1988) Geochemical and isotopic systematics in carbonatites and implications for the evolution of ocean-island sources. Geochim Cosmochim Acta 52:1–17

Olafsson M, Eggler DH (1983) Phase relations of amphibole, amphibole-carbonate, and phlogopite-carbonate peridotite: petrologic constraints on the asthenosphere. Earth Planet Sci Lett 64:305–315

Pearce TH (1990) Getting the most from your data: applications of Pearce element ratio analysis. In: Russell JK, Stanley CR (eds) Theory and application and Pearce element ratios to geochemical data analysis. Geol Assoc Can Short Course Notes 8:99–130

Richardson SH, Gurney JJ, Erlank AJ, Harris JW (1984) Origin of diamonds in old enriched mantle. Nature 310:198–202

Roeder PL, Emslie RF (1970) Olivine-liquid equilibrium. Contrib Mineral Petrol 29:275–289

Simonetti A, Bell K (1993) Isotopic disequilibrium in clinopyroxenes from nephelinite lavas from Napak volcano, eastern Uganda. Geology 21:243–246

Stacey JS, Kramers JD (1975) Approximation of terrestrial lead isotope evolution by a two-stage model. Earth Planet Sci Lett 26:207–223

Tatsumoto M (1978) Isotopic composition of lead in oceanic basalt and its implication to mantle evolution. Earth Planet Sci Lett 38:63–87

Wallace ME, Green DH (1988) An experimental determination of primary carbonatite magma composition. Nature 335:343–346

Wass SY (1979) Multiple origins of clinopyroxene in alkalic basaltic rocks. Lithos 12:115–132

Wörner G, Zindler A, Staudigel H (1984) Isotopic constraints on the chemical evoluton of the zoned Laacher See magma chamber by crystal fractionation, liquid state differentiation, magma mixing, and wall rock assimilation. In: Dungan MA, Grove TL, Hildreth W (eds) Proc ISEM Field Conf Open Magma Systems, Southern Methodist Univ, Dallas

Editorial responsibility: J. Patchett